International Tables for Crystallography (2006). Vol. F, Chapter 19.1, pp. 419–422.

19. OTHER EXPERIMENTAL TECHNIQUES

19.1. Neutron crystallography: methods and information content

BY A. A. KOSSIAKOFF

19.1.1. Introduction

Neutron and X-ray crystallography are similar in both their experimental methodologies and in the resulting information content. The principal difference between the two methods is brought about by the characteristic scattering potential of the atom types. The scattering of neutrons by material is not proportional to the atomic number, as is the case in X-ray scattering, but rather depends on the individual nuclear characteristics of each atom type. As seen in Table 19.1.1.1, these characteristics show considerably less deviation and systematic trend among the different atom types. For instance, the heavy atoms in biological material – carbon, oxygen and nitrogen – scatter with about the same magnitude as a lead or uranium atom. In addition, neutrons are scattered by the atomic nuclei, which are essentially point sources, producing diffracted intensity not attenuated by a form-factor fall-off at increasingly higher scattering angles, as is the case in X-ray diffraction (Bacon, 1975).

There are a few atomic nuclei that induce a phase change of 180° in the scattered neutron, which results in negative peaks in a neutron density map. An extremely important example of this is the hydrogen nucleus, with a scattering length of −3.7 f ($1\ \text{f} = 10^{-13}$ cm). Its isotope, deuterium, on the other hand, scatters to give positive peaks (+6.7 f). The fact that H and D atoms can be so clearly distinguished from one another has very important implications for assessing biophysical parameters, as will be discussed below.

The application of the neutron-diffraction technique, which assigns H-atom positions in proteins and differentiates between H and D atoms, has been mainly focused on structural issues in three research areas: (1) protein reaction mechanisms; (2) protein dynamics; and (3) protein–water interactions (Kossiakoff, 1985, and references therein). It must be pointed out that recent advances in nuclear magnetic resonance have made protein dynamics investigations using H/D exchange procedures much easier than similar experiments by neutron diffraction. Additionally, the advances in ultra-high-resolution X-ray crystallography, which have allowed some level of experimental determination of hydrogen atoms in proteins, have further limited the uniqueness of the neutron method. Nevertheless, a number of important structural issues that are best approached by neutron crystallography remain.

Table 19.1.1.1. *Scattering lengths for atom types*

Element	Atomic No.	Scattering length (f; $1\ \text{f} = 10^{-13}$ cm)
H	1	−3.7
D	1	6.7
C	6	6.6
N	7	9.4
O	8	5.8
Mg	12	5.2
S	16	2.8
Ca	20	4.7
Hg	80	12.7
Pb	82	9.4
U	92	8.5

19.1.2. Diffraction geometries

The general experimental setup involves use of a monochromated beam, employing normal-beam (Caine *et al.*, 1976) or flat-cone geometry (Prince *et al.*, 1978). Both approaches use flat detector surfaces, and thus there is a distortion inherent in all the diffraction phenomena that increases as a function of layer line along the axis of rotation. The extent of this effect can be calculated from the experimental parameters, but, in the case of a linear detector, there is only a moderate amount of flexibility available to make the necessary adjustments. The flat-cone geometry is well suited for a linear detector, since upper-level data fall on an undistorted plane. However, such a scheme requires that the detector be adjusted to different orientations with respect to the spectrometer axis (Prince *et al.*, 1978). In the normal-beam configuration, the crystal is usually mounted on a four-circle goniometer, allowing independent rotations around the φ, χ and ω axes to cover a full sphere of reciprocal space. This method can be efficient when used with a two-dimensional area detector because of the distortion of the diffraction pattern.

19.1.2.1. *Quasi-Laue diffractometry*

A significant advance in neutron crystallography has been the development and use of modified Laue methods to collect data (Wilkinson & Lehmann, 1991; Wilkinson *et al.*, 1992; Niimura *et al.*, 1997). These methods greatly increase the available neutron flux by using the white neutron spectrum. The full white radiation cannot be used due to very high background scattering and overlap between the diffraction peaks. A reasonable compromise between maximizing intensity while minimizing the experimental problems is to limit the white radiation component to about a 20% wavelength band by employing Ti–Ni multiple-spacing multilayers (Niimura *et al.*, 1997). In practice, the use of the Laue method in X-ray diffraction allows most of the reciprocal space to be recorded in one crystal setting. The quasi-Laue application requires several settings, depending on the neutron intensity distribution $I(\lambda)$ and the crystal symmetry. Data processing can be done using Laue software modified for neutron data.

19.1.3. Neutron density maps – information content

Fig. 19.1.3.1 illustrates several types of structural information derived from neutron density maps. Fig. 19.1.3.1(*a*) shows a well ordered tyrosine ring in the 1.4 Å structure of the protein crambin (Teeter & Kossiakoff, 1984). It can be seen that the ring hydrogen-atom locations are in positions of negative density. These peaks appear to be slightly displaced from their true positions, because the map is not at atomic resolution. At 1.4 Å, a portion of the negative peak of the hydrogen overlaps the positive peak of the ring carbon, effectively cancelling density between the atoms and giving the

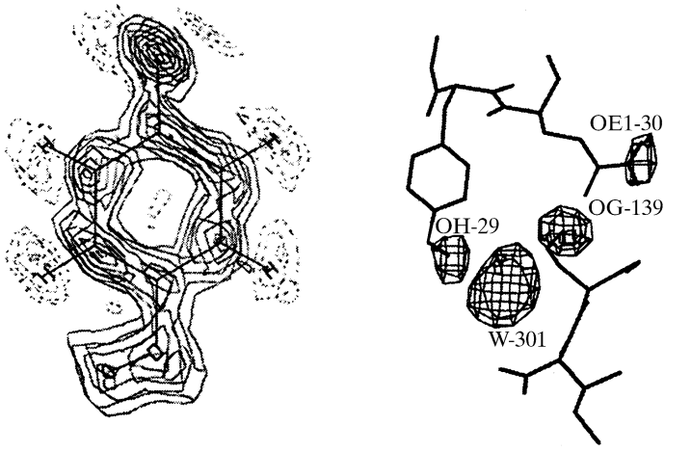

(*a*) (*b*)

Fig. 19.1.3.1. Information content in neutron density maps. (*a*) A well ordered tyrosine ring in the 1.4 Å refined structure of crambin (Teeter & Kossiakoff, 1984). (*b*) $D_2O - H_2O$ difference density map of a hydrogen-bonding network in trypsin: Gln30 Oε1–Ser139 D_γ, Ser139 O_γ–W301, W301–Tyr29 DO. Water density and H/D exchange density shown.

illusion that the peak has been translated. The hydroxyl deuterium orientation is readily determined by its position in positive density.

Use of $D_2O - H_2O$ neutron difference maps provides a high level of stereochemical information (see below) (Kossiakoff *et al.*, 1992; Shpungin & Kossiakoff, 1986). Fig. 19.1.3.1(*b*) displays a network of three hydrogen bonds involving three side-chain types and an occluded water. With knowledge of the heavy atoms alone, it is not possible to define the donor/acceptor character of any of the side chains, because they can act in either capacity, as can the water. The assignments can be made unambiguously from the $D_2O - H_2O$ density, as can the orientation of the water molecule. These maps have allowed detailed analysis of hydroxyl orientations in protein molecules (Kossiakoff *et al.*, 1990, McDowell & Kossiakoff, 1995).

Neutron diffraction is an ideal method for investigating methyl-group conformation, because it allows direct observation of hydrogen-atom positions (Fig. 19.1.3.2) (Kossiakoff & Shteyn, 1984). Although methyl groups in proteins are not held in fixed positions, but spin rapidly around their rotor axes, the time-averaged character of the diffraction experiment establishes the low-energy conformer and the degree of disorder. Accurate methyl-group analysis requires relatively higher resolution (1.5 Å or better) than characterizing other structural features.

19.1.4. Phasing models and evaluation of correctness

Neutron diffraction does not lend itself to the multiple isomorphous phasing approach. This is because the range in atomic scattering power is much narrower than for the X-ray case. There are a few relatively rare isotopes where a significant anomalous effect exists; however, they are not adequate for getting primary phasing information (Schoenborn, 1975). In practice, the initial phasing model has to be derived from the X-ray-determined structure. This is done by applying the appropriate neutron scattering lengths to the refined X-ray coordinates (Norvell & Schoenborn, 1976). Thus, at least in the early stages of analysis, the neutron model relies heavily on the accuracy of the X-ray structure. The importance of an accurate phasing model is borne out by the fact that in several investigations the phasing models were not accurate enough to allow the structure to be refined successfully.

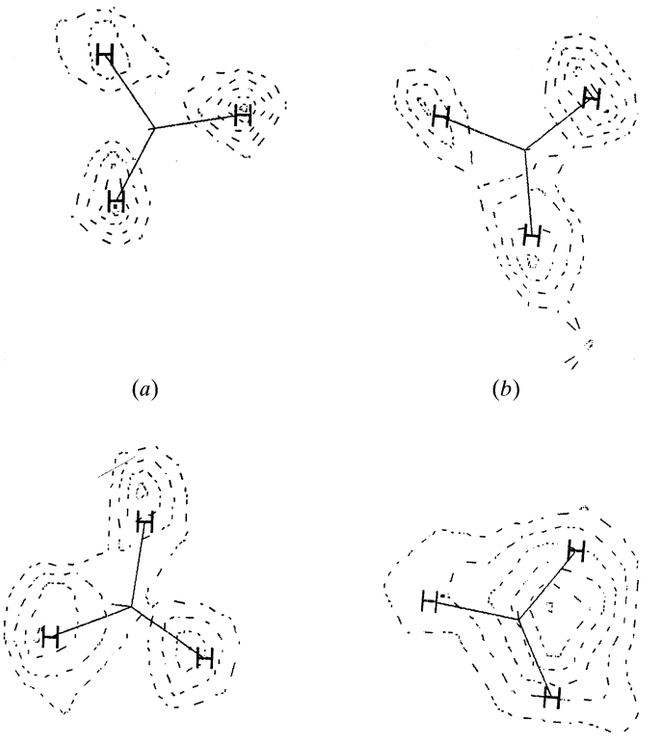

(*a*) (*b*) (*c*) (*d*)

Fig. 19.1.3.2. Sections of a neutron difference Fourier map showing methyl hydrogen densities for several representative methyl groups. No phasing information about the methyl hydrogens was included in the model; therefore, hydrogens should appear in the difference map at their true positions but at reduced density (∼ half weight). The groups shown are: (*a*) Ala24, (*b*) Thr21, (*c*) Thr28, and (*d*) Ala45.

19.1.5. Evaluation of correctness

It is an important first step in the structural analysis to determine the quality of the phases derived from the X-ray structure (Kossiakoff, 1983). Several methods have been used. Using the initial phasing model, the most powerful tests examine an unbiased neutron Fourier map for the appearance of features that are independent of the model. The presence or absence of these features, especially those resulting from the scattering of hydrogen and deuterium atoms, is the most reliable measure of the phasing model. One such test is to evaluate the appearance of the water structure, *i.e.*, the water molecules hydrogen-bonded to the surface of the protein. The water molecules observed in the X-ray analysis are excluded from the neutron-phasing model. The test is applied in cases where the crystals have been soaked in D_2O. The peaks in the neutron density map that correspond to the strongly coordinated water-molecule positions owe their existence solely to the neutron data and phasing model. Even at an early stage, because of the large neutron-scattering potential of D_2O, many of these tightly bound waters found in the X-ray structures should also be observable in the neutron density map.

Another aspect to test phasing reliability is the ability to identify the orientation of side-chain amide groups of asparagine and glutamine. The difference in neutron scattering between O and the two deuteriums and the Nδ2 (5.8 f *versus* 22.6 f) is large enough to be detectable in the Fourier map when these groups are well ordered (Fig. 19.1.5.1). The use of unexchangeable hydrogens for evaluation is considerably more complicated, despite the fact that they constitute about one-half the total number of atoms in the molecule. The difficulty arises from the negative scattering character of the hydrogens, which displaces their apparent positions

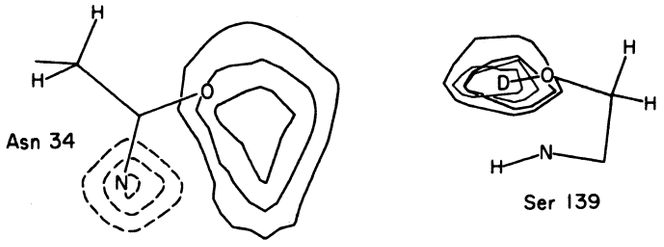

(*a*) (*b*)

Fig. 19.1.5.1. Difference map of Asn34 in the trypsin structure. (*a*) In a protein X-ray analysis, the difference in scattering intensity between O and NH_2 is much too small to be detected. In contrast, the neutron-scattering magnitudes of oxygen and nitrogen (5.8 f versus 9.4 f) are quite dissimilar, and there is additional scattering at the nitrogen site from the two bound deuterium atoms. The resulting differential is over 350%, quite large enough to be detected for well ordered side chains. The nitrogen and oxygen positions shown are from the X-ray model. The difference density indicates that the orientation of the nitrogen and oxygen atoms is incorrect and should be rotated by 180° around the C_β–C_γ bond. (*b*) Difference map for Ser139. On well ordered hydroxyl side chains, the orientation of deuterium atoms can sometimes be assigned.

in the Fourier map from the true positions and, coupled with their short bond lengths, complicates the interpretation of the results. Additionally, it has been shown that small errors in positional and thermal parameters of the parent atoms can further complicate the identification of hydrogen-atom positions (Kossiakoff & Spencer, 1981).

19.1.6. Refinement

The methodologies employed to refine neutron data are essentially the same as those used in most X-ray studies. These include real-space (Hanson & Schoenborn, 1981; Norvell & Schoenborn, 1976; Schoenborn & Diamond, 1976), reciprocal-space (Bentley & Mason, 1980; Phillips, 1984; Wlodawer & Hendrickson, 1982; Wlodawer & Sjolin, 1981) and restrained difference-map refinement (Kossiakoff & Spencer, 1980; 1981). A joint refinement technique in which the neutron and X-ray data are refined simultaneously has been developed (Wlodawer & Hendrickson, 1982). In addition to the normal difficulties encountered in the refinement of any protein structure, there are several that are peculiar to the neutron-diffraction technique. These special problems arise from the close proximity of hydrogen atoms to their parent atoms, coupled with the effects of the negative scattering length of the hydrogen atoms. Potential problems exist when the difference density generated from positional errors of one atom overlaps an adjacent atom site. The situation is further complicated by the fact that, because of its negative scattering length, an error in a hydrogen-atom position is minimized by moving the atom down the gradient, that is, in the opposite direction to that required for correcting parent-atom positions. To evaluate the extent of this problem in refinement, a test was devised using a 2.2 Å data set (Kossiakoff & Spencer, 1981). The coordinates of the protein trypsin were perturbed by a varying, but known, amount from their ideal positions. It was determined that, in general, convergence towards the true coordinate could be obtained when the coordinate errors were less than 0.3 Å; however, if the parent atom (an atom with one or more hydrogens attached to it) was displaced by more than 0.6 Å from its correct position, the effect of neighbouring hydrogens rendered the calculated shifts inaccurate. The results of this study support the observations of other investigators that it is absolutely crucial that the starting phasing model be of high quality, because the range of convergence of a neutron analysis is relatively small.

19.1.7. D_2O – H_2O solvent difference maps

D_2O – H_2O solvent difference maps provide an unbiased method for identifying water molecules and exchangeable hydrogens (Kossiakoff *et al.*, 1992). For several years, the large difference in the scattering characteristics of neutrons by H_2O compared to D_2O has been effectively exploited by using density matching and exchange labelling in small-angle neutron-scattering experiments. This difference can likewise be exploited in neutron protein crystallography to determine the detailed structural characteristics of protein hydration through the calculation of solvent difference maps (Shpungin & Kossiakoff, 1986; Kossiakoff *et al.*, 1992). In practice, such maps are obtained by comparing the changes in diffracted intensities between two sets of data – one obtained from a crystal having H_2O as the major solvent constituent, and a second where D_2O is the solvent medium. To a good approximation, the protein-atom contributions to the scattering intensities in both data sets are equal and cancel, but since H_2O and D_2O have very different scattering properties, their differences are accentuated to reveal an accurate and nearly unbiased representation of the solvent structure.

The features of a solvent difference map of this type are not as affected by errors in the phasing model as conventional difference Fourier maps. In addition, there are refinement procedures that can be applied to them that lead to significant enhancement in signal/noise discrimination. The basic feature of the method is a set of density-modification steps based on the fact that a considerable amount of information about the density distribution of the crystallographic unit cell is known. For instance, it is known that

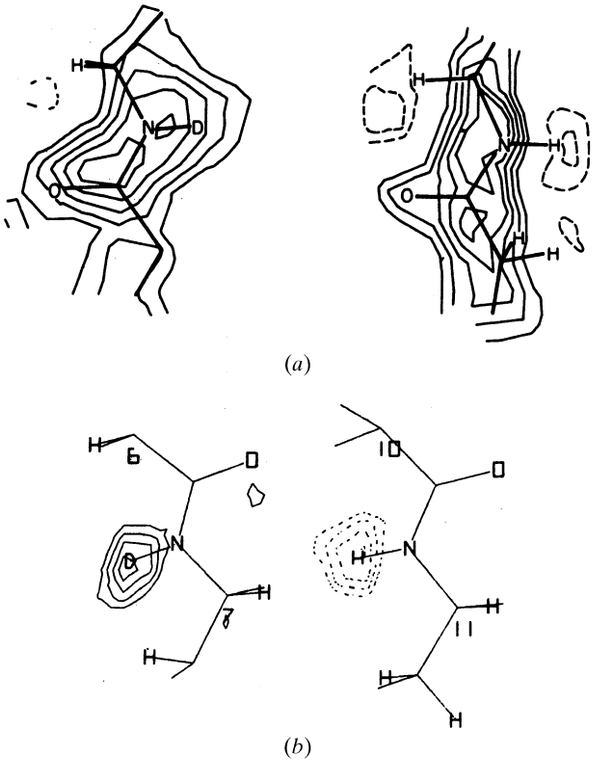

(*a*)

(*b*)

Fig. 19.1.8.1. Sections of neutron density maps taken in the plane of the peptide group. (*a*) $2F_o - F_c$ maps showing an example of an exchanged and unexchanged amide peptide group. (*b*) $D_2O - H_2O$ difference density map showing the same.

the region of the unit cell occupied by protein atoms should be featureless in solvent maps. It can also be assumed that, as an approximation, solvent regions further than 4 Å from the protein surface have bulk solvent characteristics and can be treated as a constant density region. Combining these two regions gives about 50–60% of the total volume of the unit cell.

Knowledge of the density content of such a large percentage of the unit cell places a strong constraint on the overall character of the Fourier transform, a fact that can be used to improve the quality of the experimentally determined phases

19.1.8. Applications of $D_2O - H_2O$ solvent difference maps

19.1.8.1. *Orientation of water molecules*

In the case of a highly ordered water in a $D_2O - H_2O$ difference map, the oxygen scattering components will cancel (having identical locations and scattering potential), but because H and D have very different scattering properties (H = −3.8 f, D = +6.7 f), large peaks will be found in the map at the D − H positions. Consequently, these ordered waters can usually be oriented with reasonable accuracy in maps better than 2.0 Å resolution (see Fig. 19.1.3.1*b*).

19.1.8.2. *H/D exchange*

Fig. 19.1.8.1 shows examples of density around exchanged and unexchanged amide peptide sites. The density in Fig. 19.1.8.1(*a*) is characteristic of $2F_o - F_c$ Fourier maps; the D is in positive density, extending off the peptide nitrogen, and the H is represented by negative density, separated and translated off the nitrogen. Fig. 19.1.8.1(*b*) shows a $D_2O - H_2O$ density map at the same resolution (2.0 Å). Assignment of H/D character is unambiguous, and it is possible to evaluate partial exchange properties more reliably.

(Wüthrich & Wagner, 1975) was a genuine surprise for the following reasons. In the refined X-ray crystal structure of BPTI, the aromatic rings of phenylalanine and tyrosine are among the side chains with the smallest temperature factors. For each ring, the relative values of the *B* factors increase toward the periphery, so that the largest positional uncertainty is indicated for carbon atom 4 on the symmetry axis through the C^{β}—C^{1} bond, rather than for the carbon atoms 2, 3, 5 and 6 (Fig. 19.7.5.1), which undergo extensive movements during the ring flips. Theoretical studies then showed that the crystallographic *B* factors sample multiple rotation states about the C^{α}—C^{β} bond, whereas the ring flips about the C^{β}—C^{1} bond seen by NMR are very rapid 180° rotations connecting two indistinguishable equilibrium orientations of the ring. The *B* factors do not manifest these rotational motions because the populations of all non-equilibrium rotational states about the C^{β}—C^{1} bond are vanishingly small. The ring-flip phenomenon is now a well established feature of globular proteins, manifesting ubiquitous low-frequency internal motions with activation energies of 60–100 kJ mol^{-1}, amplitudes of $\gtrsim$1.0 Å and activation volumes of about 50 $Å^3$ (Wagner, 1980), and involving concerted displacement of numerous groups of atoms (Fig. 19.7.5.1).

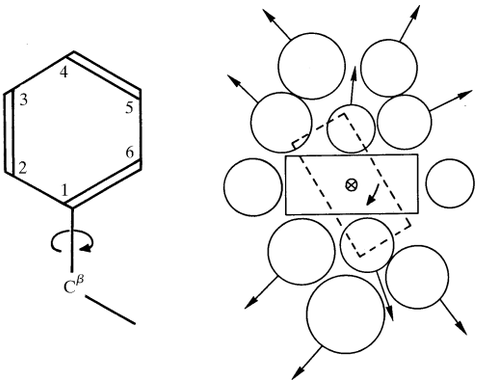

Fig. 19.7.5.1. 180° ring flips of tyrosine and phenylalanine about the C^{β}—C^{1} bond. On the left, the atom numbering is given and the χ^2 rotation axis is identified with an arrow. The drawing on the right presents a view along the C^{β}—C^{1} bond of a flipping ring in the interior of a protein, where the broken lines indicate a transient orientation of the ring plane during the flip. The circles represent atom groups near the ring, and arrows indicate movements of atom groups during the ring flip (Wüthrich, 1986).

References

19.1

Bacon, G. E. (1975). *Neutron diffraction*, pp. 155–188. Oxford: Clarendon Press.

Bentley, G. A. & Mason, S. A. (1980). *Neutron diffraction studies of proteins. Philos. Trans. R. Soc. London Ser. B*, **290**, 505–510.

Caine, J. E., Norvell, J. C. & Schoenborn, B. P. (1976). *Linear position-sensitive counter system for protein crystallography. Brookhaven Symp. Biol.* **27**, 43–50.

Hanson, J. C. & Schoenborn, B. P. (1981). *Real space refinement of neutron diffraction data from sperm whale carbonmonoxymyoglobin. J. Mol. Biol.* **153**, 117–146.

Kossiakoff, A. A. (1983). *Neutron protein crystallography: advances in methods and applications. Annu. Rev. Biophys. Bioeng.* **12**, 259–282.

Kossiakoff, A. A. (1985). *The application of neutron crystallography to the study of dynamic and hydration properties of proteins. Annu. Rev. Biochem.* **54**, 1195–1227.

Kossiakoff, A. A., Shpungin, J. & Sintchak, M. D. (1990). *Hydroxyl hydrogen conformations in trypsin determined by the neutron solvent difference map method: relative importance of steric and electrostatic factors in defining hydrogen-bonding geometries. Proc. Natl Acad. Sci. USA*, **87**, 4468–4472.

Kossiakoff, A. A. & Shteyn, S. (1984). *Effect of protein packing structure on side-chain methyl rotor conformations. Nature (London)*, **311**, 582–583.

Kossiakoff, A. A., Sintchak, M. D., Shpungin, J. & Presta, L. G. (1992). *Analysis of solvent structure in proteins using neutron $D_2O - H_2O$ solvent maps: pattern of primary and secondary hydration of trypsin. Proteins Struct. Funct. Genet.* **12**, 223–236.

Kossiakoff, A. A. & Spencer, S. A. (1980). *Neutron diffraction identifies His 57 as the catalytic base in trypsin. Nature (London)*, **288**, 414–416.

Kossiakoff, A. A. & Spencer, S. A. (1981). *Direct determination of the protonation states of aspartic acid-102 and histidine-57 in the tetrahedral intermediate of the serine proteases: neutron structure of trypsin. Biochemistry*, **20**, 6462–6474.

McDowell, R. S. & Kossiakoff, A. A. (1995). *A comparison of neutron diffraction and molecular dynamics structures: hydroxyl group and water molecular orientations in trypsin. J. Mol. Biol.* **250**, 553–570.

Niimura, N., Minezaki, Y., Nonaka, T., Castagna, J.-C., Cipriani, F., Hoghoj, P., Lehmann, M. S. & Wilkinson, C. (1997). *Neutron Laue diffractometry with an imaging plate provides an effective data collection regime for neutron protein crystallography. Nature Struct. Biol.* **4**, 909–914.

Norvell, J. C. & Schoenborn, B. P. (1976). *Use of the tangent formula for the refinement of neutron protein data. Brookhaven Symp. Biol.* **27**, 1124–1130.

Phillips, S. E. V. (1984). *Hydrogen bonding and exchange in oxymyoglobin*. In *Neutrons in biology*, edited by B. P. Schoenborn, pp. 305–322. New York: Plenum Press.

Prince, E., Wlodawer, A. & Santoro, A. (1978). *Flat-cone diffractometer utilizing a linear position-sensitive detector. J. Appl. Cryst.* **11**, 173–178.

Schoenborn, B. P. (1975). *Anomalous scattering*. In *Conference on anomalous scattering*, edited by S. Rameseshan & S. C. Abrahams, pp. 407–421. Copenhagen: Munksgaard.

Schoenborn, B. P. & Diamond, R. (1976). *Neutron diffraction analysis of metmyoglobin. Brookhaven Symp. Biol.* **27**, 3–11.

Shpungin, J. & Kossiakoff, A. A. (1986). *A method of solvent structure analysis for proteins using $D_2O - H_2O$ neutron difference maps. Methods Enzymol.* **127**, 329–342.

Teeter, M. M. & Kossiakoff, A. A. (1984). *The neutron structure of the hydrophobic plant protein crambin*. In *Neutrons in biology*, edited by B. P. Schoenborn, pp. 335–348. New York: Plenum Press.

Wilkinson, C., Gabriel, A., Lehmann, M. S., Zemb, T. & Ne, F. (1992). *Image plate neutron detector. Proc. Soc. Photo-Opt. Instrum. Eng.* **1737**, 324–329.

Wilkinson, C. & Lehmann, M. S. (1991). *Quasi-Laue neturon diffractometer*. *Nucl. Instrum. Methods A*, **310**, 411–415.

Wlodawer, A. & Hendrickson, W. A. (1982). *A procedure for joint refinement of macromolecular structures with X-ray and neutron diffraction data from single crystals. Acta Cryst.* A**38**, 239–247.

Wlodawer, A. & Sjolin, L. (1981). *Orientation of histidine residues in RNase A: neutron diffraction study. Proc. Natl Acad. Sci. USA*, **78**, 2853–2855.

19.2

Amos, L. A., Henderson, R. & Unwin, P. N. (1982). *Three-dimensional structure determination by electron microscopy of two-dimensional crystals*. *Prog. Biophys. Mol. Biol.* **39**, 183–231.